Dipl.-Ing. (FH)
Alexander Zarschler,
Bad Hersfeld

Development of Centrifugal Plug-in Fan Impellers

Demands on energy efficiency and hygienic properties of central air handling units are becoming increasingly exacting, and fans are no exception to this rule. In recent years, technology of central air handling units has been dominated by direct-driven plug-in fans with backward-curved blades, not least because of their economic efficiency. These units meet the demands of AHU system manufacturers for energy-optimized, compact yet powerful air-moving devices.

Advantages of plug-in fans

Key advantages of direct-driven plug-in fans compared to belt-driven fans may be summarized as follows:

Fans with spiral casing are typically driven via a V-belt which imposes a fixed operating speed (rpm). On systems without frequency converter, subsequent adjustments of the operating point or rotational speed can usually be made only by replacing the pulleys. But even where belt-driven fans are speed-controlled by a frequency converter, the plug-in fan proves to be a superior solution since the belt drive is a “high wearing” component requiring frequent maintenance.

The maintenance-free plug-in fan, on the other hand, lends itself perfectly to the infinitely variable rpm control provided by frequency conversion. Experience has shown that this technology yields substantial energy savings. Moreover, the use of a plug-in fan eliminates the belt losses which may greatly impair the overall efficiency of the drive system. Negative factors such as inlet and outlet conditions, bearing supports, V-belts, pulleys, belt guards, baffle plates, etc.,

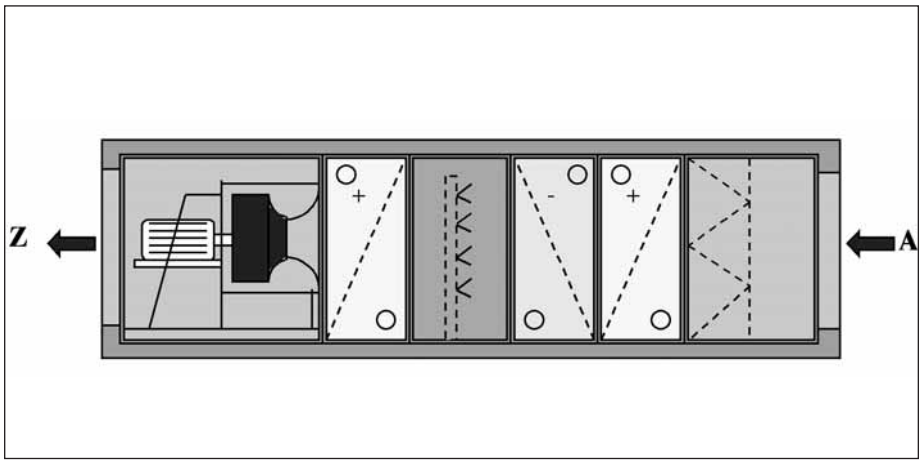

Fig. 1: Central air handling unit

which interfere with an optimum airflow to the impeller, are practically eliminated by plug-in fans. These energy efficiency benefits are particularly obvious at small pressure increases. (Fig. 2)

In certain cases the absence of the belt drive can even eliminate the need for a second filter stage at the fan outlet. Since there is no problem with abraded belt particles, a single inlet-side filter will usually suffice [1].

Another advantage of plug-in fans is the fairly low discharge airspeed on the fan outlet side. The resulting low share of dynamic pressure in the total pressure head is a particular powerful argument in favor of a plug-in fan. This advantage makes itself felt specifically at low system pressures where the dynamic element in the overall pressure increase is fairly high.

Moreover, the above-described elimination of bearing braces and V-belt pulleys permits highly accurate volume flow measurements acrosss the inlet nozzle. By determining the pressure difference between the fan inlet

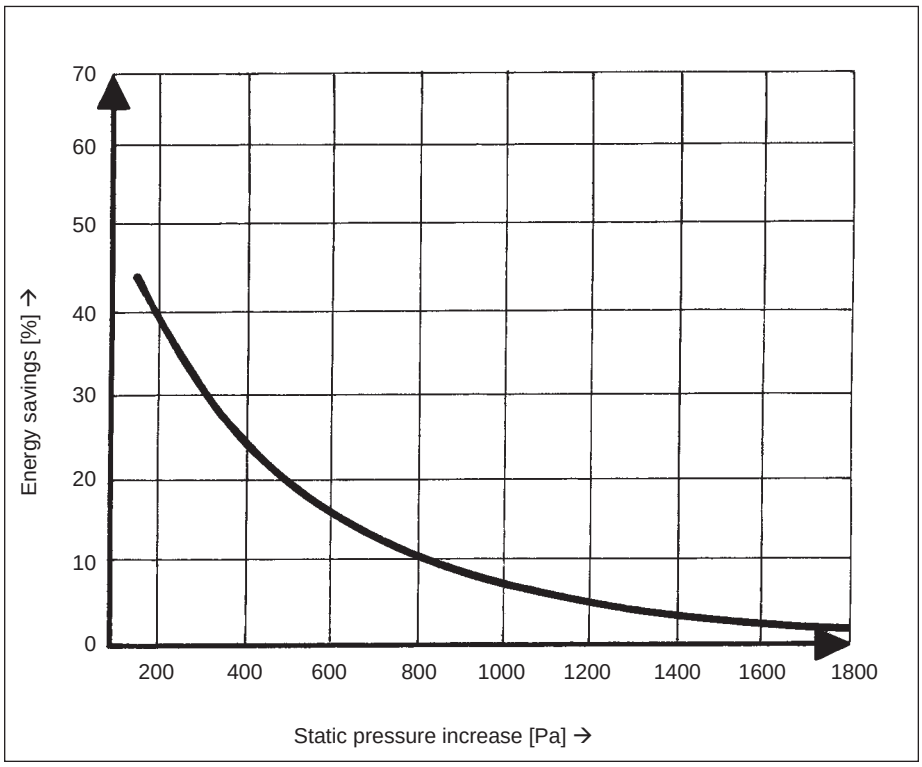

Fig. 2: Energy saving potential versus static pressure increase

chamber and the narrowest point of the nozzle, it is possible to determine the volumetric throughput with a tolerance of ± 5% using an empirical coefficient.

Demands on the impeller

Since plug-in fans are mostly designed for use in central air handling units, their appearance, geometry and performance ranges are naturally dictated by the demands of this application. The criteria important to the equipment manufacturer shall be discussed in detail below.

One major success factor for an AHU impeller is compact design. In other words, the impeller should cover the broadest possible output range while being itself of minimum dimensions. Meeting this dual requirement will translate into tangible benefits such as low purchasing cost, reduced space needs and improved hygiene properties.

11

The versatility and hence, the cost-efficiency of an air handling unit are naturally a function of the correlation between output capacity, sound emission and mechanical load resistance (max. rpm level).

It follows that the impeller should be able to perform at high peak efficiency levels over a broad volume flow range. In other words, it will hardly help the manufacturer to have an impeller with a peak efficiency way in excess of 70% if this performance is only achieved within a narrow throughput bracket (Fig. 3). AHU system manufacturers demand impellers whose efficiency will not drop excessively from the optimum point on either side of the volume flow spectrum.

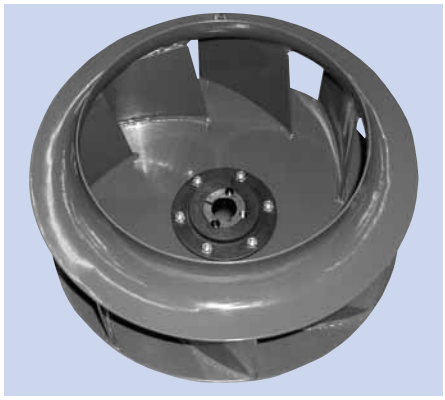

Fig. 3: New development of a plug-in fan with a high performance density at TLT-Turbo GmbH

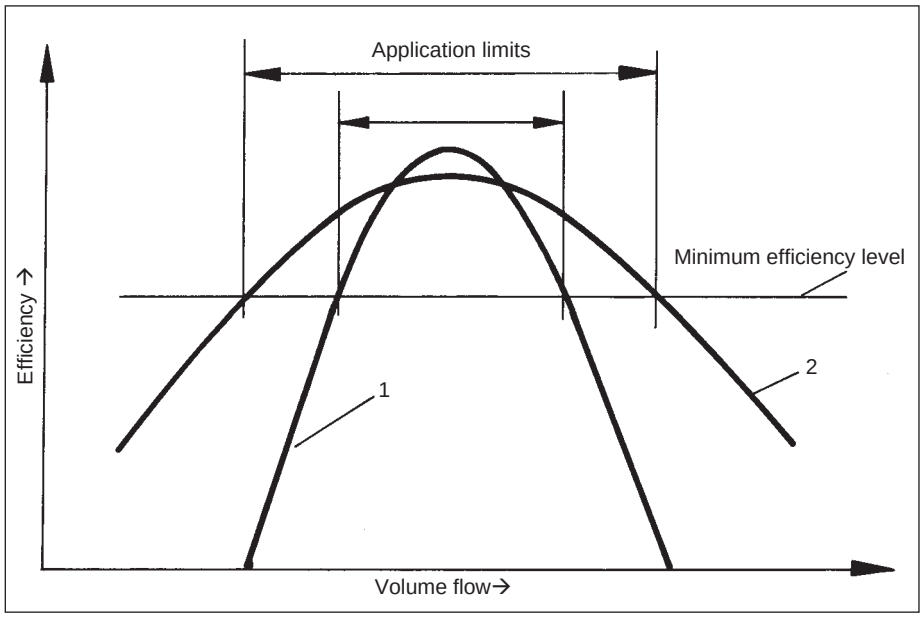

Fig. 4
Diagram: Application limits of two centrifugal fan impellers
Impeller 1: Very high efficiency, small application range
Impeller 2: High efficiency, broad application range

To avoid extra cost of downstream sound damping, noise emissions of an impeller merits particular attention. Care should be taken to ensure that a high efficiency is achieved in conjunction with the lowest possible acoustic output.

Another important point for the manufacturer is the impeller's mechanical load resistance. Due to the improved control capabilities that became available with the advent of frequency converters, today's impellers are operated over a broad rpm range. Indeed, they are often run in conditions bringing them close their mechanical strength limits.

Development of a new impeller

Each new impeller development is dominated initially by the main criteria outlined above. Although fans are standardized, volume-produced items today, each fan must be optimally adapted to the customer's application needs.

To achieve this objective, the use of appropriate development software has become indispensable. In addition, designers are using diverse computing programs, CAD systems, FEM (finite element method) stress analysis and CFD (computational flow dynamics) systems; particularly the latter two have become increasingly widespread in recent years. They allow the user to simulate entire fans or fan segments in the computer for the purposes of fluid-mechanical analysis. On the basis of Navier-Stokes equations, fluid flows can be described by mathematical expressions. This makes it possible to compute relevant parameters such as velocity, pressure, density, temperature, etc. With the aid of these tools, different design variants can be modelled and interference factors can be eliminated in advance.

FEM stress analysis is employed to verify the selected impeller design for its static, dynamic and fracture-mechanical strength as well as its thermal resistance. Key dimensioning data are thus obtained. Use of these various software tools accelerates product development times significantly. But despite the range of sophisticated computer-based fan dimensioning and optimizing techniques available today, the engineer must still rely on

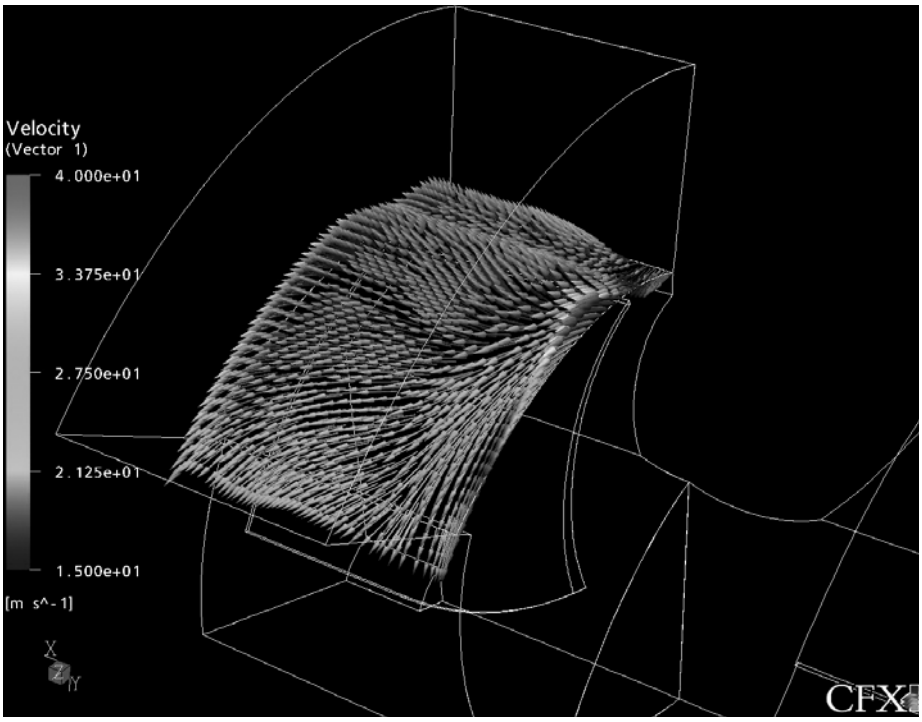

Fig. 5: Velocity vectors on top blade surface calculated by CFD

traditional calculating methods, fabricated prototypes, practical measurements and, not least significally, empirical findings. One time-saving calculating method which has been found particularly useful in this context is the one-dimensional Eulerian stream filament theory. This technique can describe the rather complex airflow conditions between impeller inlet and blade exit on the basis of a single stream filament having a mean velocity that is a function of the volumetric flow rate and the cross-section of the flow channel [2].

As mentioned earlier, the impellers considered here are expected to combine the broadest possible output range with minimum physical dimensions.

Flow coefficient (1)

$$\varphi = \frac{\dot{V} \cdot 4}{u_2 \cdot \pi \cdot d_2^2}$$

The flow coefficient - also referred to as discharge coefficient - describes the ratio between actual and theoretically achievable flow (product of the impeller's circular area and the tip velocity).

Head coefficient (2)

$$\psi = \frac{\Delta p \cdot 2}{\rho \cdot u_2^2}$$

The pressure coefficient - or head coefficient - relates the static pressure delivered by the impeller to its tip velocity pressure equivalent.

Efficiency (3)

$$\eta = \frac{\dot{V} \cdot \Delta p}{P_w}$$

The efficiency is the ratio of power gained by the fluid to the input of shaft power supplied.

The efficiency of plug-in fans examined here should vary between 60 and over 70% for central AHU applications. The aim is to attain a high capacity coefficient φ and a high pressure head coefficient ψ at the same time. Assuming the optimum efficiency η_{opt} described above as an approximately constant factor, the following can be defined with regard to the objective of maximizing air flow while minimizing impeller dimensions:

The product of the flow coefficient φ and the head coefficient ψ must be as large as possible.

This product is referred to as power density.

Power density (4)

$$= \varphi \cdot \psi$$

The aim of TLT-Turbo GmbH's research efforts, therefore, was to develop a direct-driven plug-in fan having a maximum power density in the efficiency range described above. Power density at the optimum point can be increased, according to equation (4), by raising head coefficient ψ and flow coefficient φ.

Options for increasing the head coefficient:

According to [3], the head coefficient of impellers with backward-curved blades can be raised by increasing the blade angle β_2. However, this increase has its natural limits. If the number of blades is kept constant, raising the blade exit angle may result in flow separation due to higher blade loads on the blade suction side. The separation that occurs as the axial flow is deflected into a centrifugal flow (meridian flow) reduces the pressure increase and hence, the impeller's efficiency. It follows that an increase of the blade exit angle and hence, of the head coefficient ψ, can only be achieved by raising the number of blades z, thus keeping the blade load and the

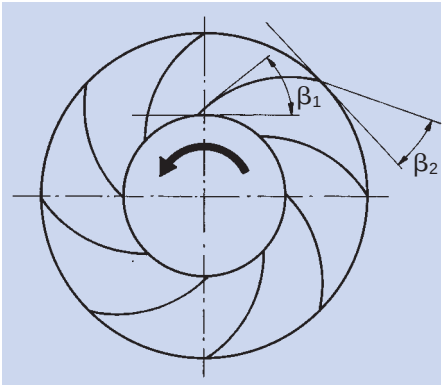

Fig. 6: Sectional view of a plug-in fan with backward-curved blades
Blade exit angle β_2 and blade inlet angle β_1

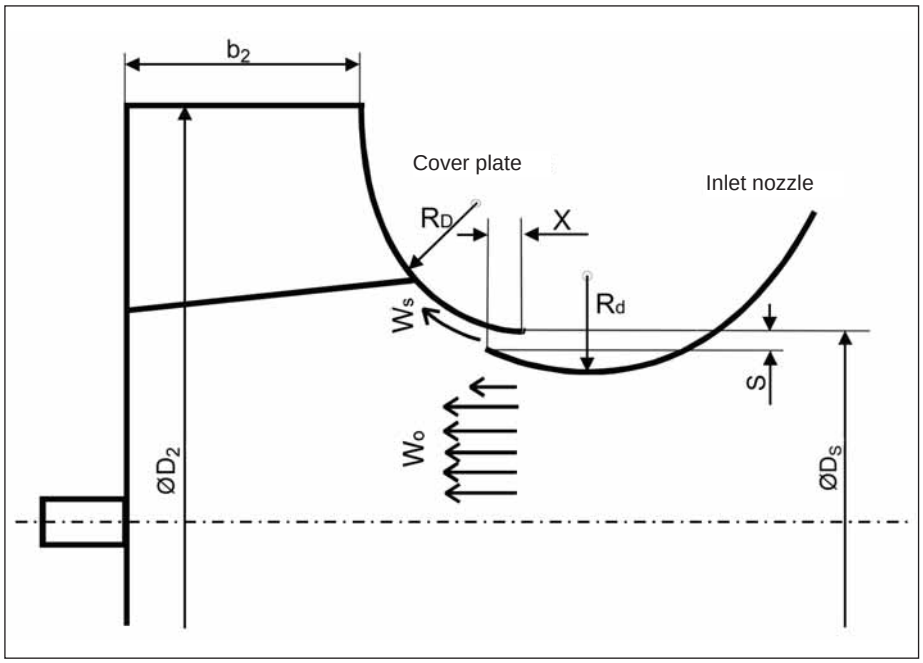

Fig. 7: Median section through a plug-in fan impeller

associated flow separation effects within acceptable limits. On the other hand, providing more blades will create a greater boundary layer friction in the blade channel (inherent loss).

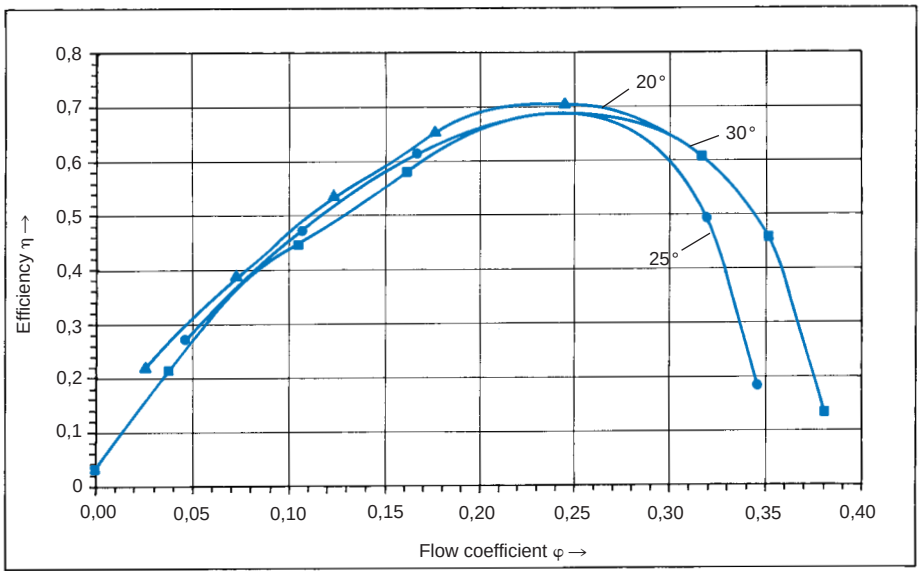

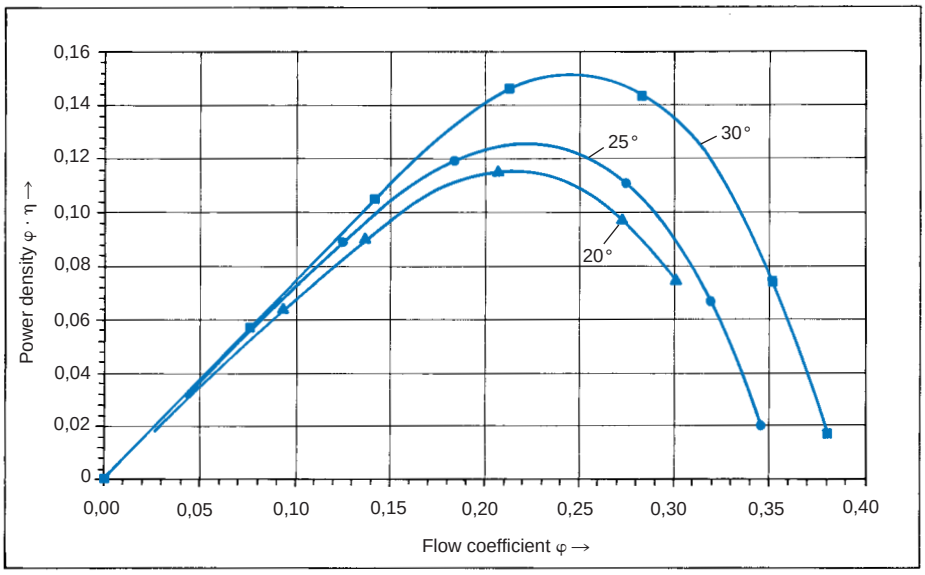

Fig. 8
Impellers with a width ratio $D_2/b_2 = 4.2$
Efficiency and power density versus flow coefficient for various blade exit angles.
1) Blade exit angle $\beta_2 = 20°$
2) Blade exit angle $\beta_2 = 25°$
3) Blade exit angle $\beta_2 = 30°$

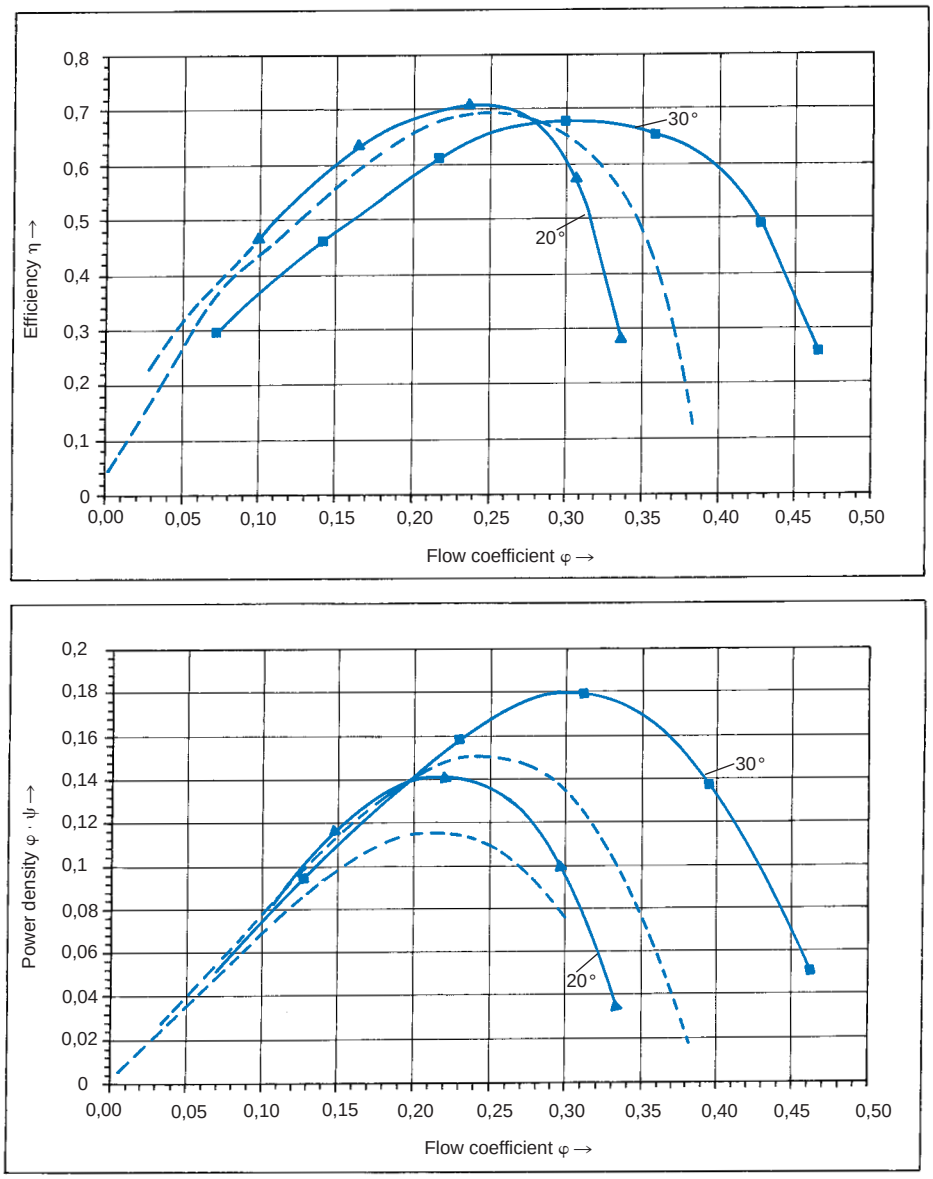

Fig. 9
Impellers with a width ratio $D_2/b_2 = 3.5$
Efficiency and power density versus flow coefficient for various blade exit angles.
1) Blade exit angle $\beta_2 = 20°$
2) Blade exit angle $\beta_2 = 30°$
The grey dashed line marks the corresponding values for a width ratio $D_2/b_2 = 4.2$

Options for increasing the flow coefficient

The most straightforward method of increasing the impeller's absorption capacity and hence, the flow coefficient φ is to increase the impeller width b. The impeller throughput will rise in proportion to this blade width increase. Again, needless to say, the blade width cannot be raised at will since the need for a separation-free airflow and the impeller's mechanical strength impose certain physical limits. Beyond a certain D_2/d_2 width ratio, the flow becomes detached from the blade surface in the meridian cross-section, resulting in a corresponding drop in the head coefficient, flow coefficient and impeller efficiency.

From this point onwards, flow attachment to the blade surface can only be ensured to a certain degree by optimizing the gap intake ratio s/D_S to increase the gap velocity. The gap air is then returned tangentially toward the impeller cover plate, causing low-energy boundary layers to be enriched with additional discharge air and stabilizing the flow as it is deflected [2]. The effectiveness of the gap jet in assisting flow deflection depends on the optimum velocity ratio w_S/w_0. As power density is progressively raised by increasing the flow coefficient φ, head coefficient ψ is bound to decrease slightly. Given the weaker gap impulse resulting from this static pressure drop, the gap velocity ratio W_S/W_0 is reduced accordingly. As a result, the now more unfavourable ratio W_S/W_0 between gap velocity and basic velocity will again give rise to flow separation once a given threshold is exceeded.

The high impact of the above parameters on fan performance shows how much importance must be attached to a meticulous design of the inlet nozzle contour, gap overlap (X), gap width (S), and contour of the cover plate.

The next stage in the development process was the design calculation of various impellers and the fabrication of corresponding prototypes. To determine the influence of the individual parameters, impellers with a width ratio $D_2/b_2 = 4.2$ and blade exit angles β_2 of 20, 25 and 30 degrees were tested as a first step.

To account for the higher blade loads, the impeller with the $\beta_2 = 30°$ exit angle was equipped with z = 8 blades. For the remaining impellers, a number z = 6 blades was adopted.

Fig. 8 clearly shows the rise in power density that accompanies the increase in the blade exit angle β_2. As the power density increases, a slight drop in efficiency can be observed, amounting to 1 - 1.5% at the optimum point. However, this is more than offset by the power gain achieved at the peak efficiency point, which is 21% in the case of 25° impeller and even 31% for the 20° impeller.

In a second development step, an increase in blade width was implemented. The width ratio used here, viz., $D_S/b_2 = 3.5$, corresponds approximately to a 20% increase in blade width.

Fig. 9 demonstrates the resulting substantial increase in power density at the optimum efficiency level. The 30° impeller with widened blades covers a much wider performance range

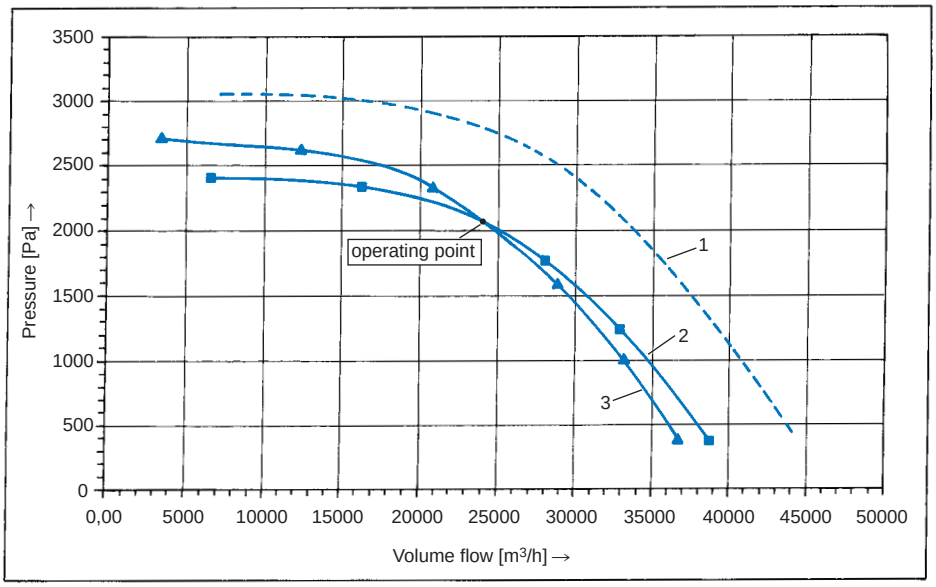

Fig. 10
Comparison of a conventional plug-in fan impeller to ER 30/3.5 at the same operating point.
V = 23000 m?/h, dpt = 2100 Pa
1) 30/3.5 at 2225 rpm
2) ER 30/3.5 at 1950 rpm (reduced rotational speed)
3) Reference wheel of same nominal size at 2225 rpm

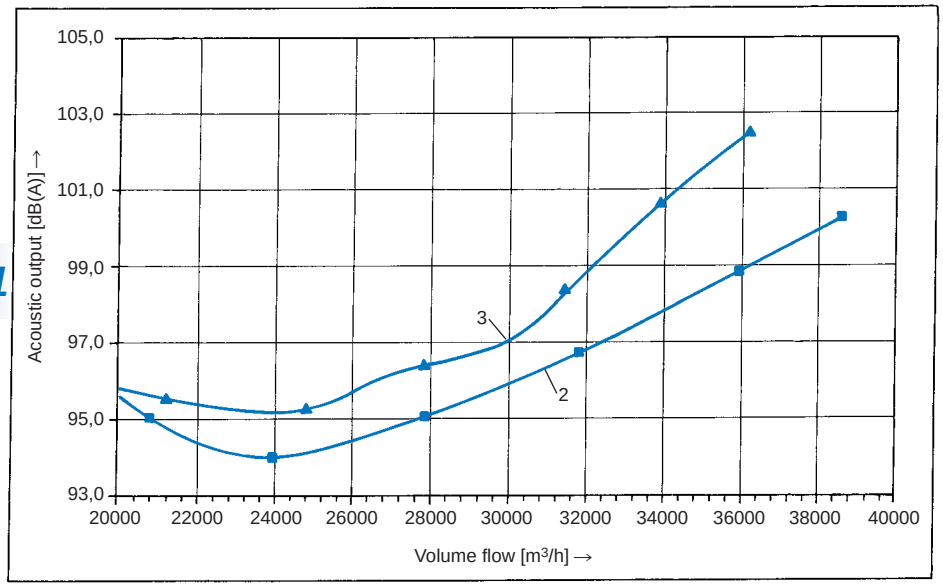

11

ting point to be attained with a unit that is one full design size smaller (Fig. 11).

than all other impellers. The efficiency loss of about 2.5% is only small when compared to the 28% gain in power density.

From an acoustic perspective, too, the plug-in fan shows very favourable chacteristics. The A-weighted sound pressure level at identical rpm corresponds to that of conventional plug-in fans. However, a major benefit is achieved in terms of its superior absorption capacity, i.e. at the same operating point, the ER 30/3.5 unit can be run at much lower rpm than comparable impellers. This translates into a reduced acoustic power output (Fig. 10).

Compared directly to conventional open-running impellers, the ER 30/3.5 even allows the same opera-

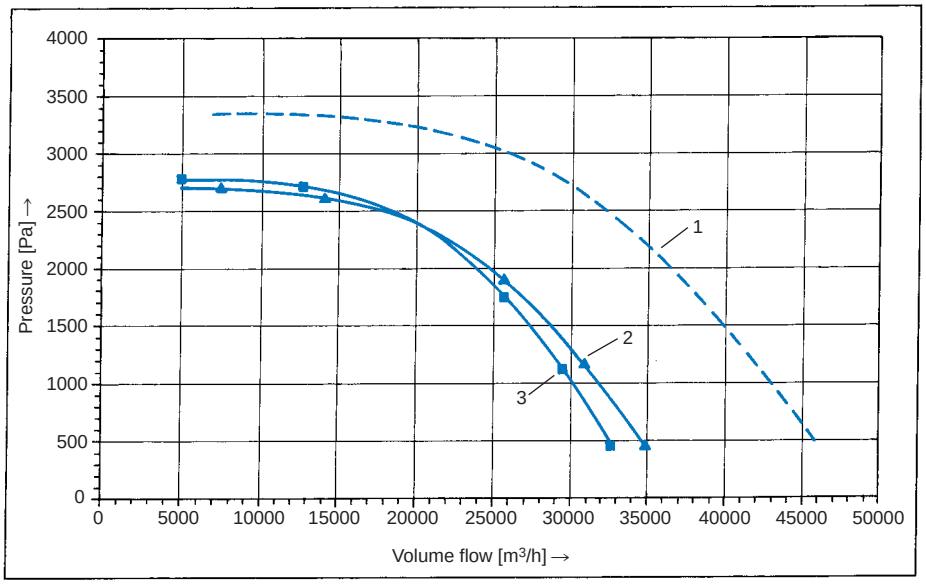

Fig. 11 Nominal size (NG) reduction from NG 710 to NG 630 at the same operating point.
1) ER 30/3.5, NG 710
2) Conventional centrifugal impeller
3) ER 30 3.5, NG 630

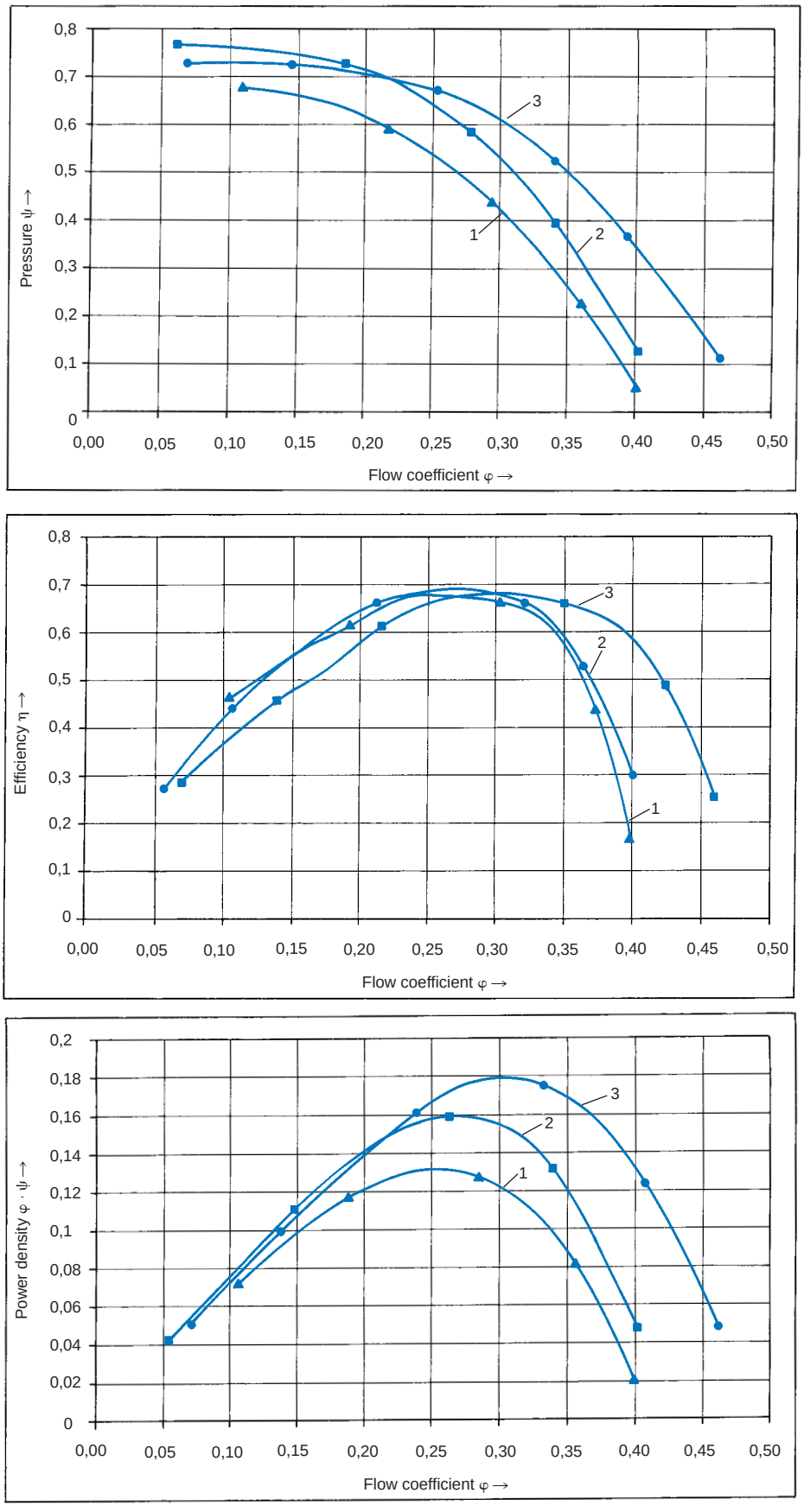

Fig. 12
Comparison of ER 30/3.5 characteristic curves with impellers from diverse manufacturers
1) Reference impeller 1
2) Reference impeller 2
3) ER 30/3.5

A comparison (Fig. 12 and 13) of the newly developed open-running centrifugal impeller ER30/3.5 with other impellers currently marketed shows that the new design attains much higher power densities at a constant efficiency. The initially defined goal of developing a high-power-density plug-in impeller for use in AHU equipment has thus been achieved.

Optimization of the impeller inlet (gap width s and gap overlap x)

As outlined in the previous section, the optimization of the impeller inlet contour in conjunction with the existing cover plate contour was a factor to which great importance was attached during development of this impeller. An impeller inlet nozzle matched exactly to the centrifugal impeller is vastly important for an appropriate flow behaviour in the median cross-section, since naturally, the risk of flow separation is greatest in the area of deflection from axial to centrifugal flow. To avoid this effect and to find the optimum wheel inlet geometry, various inlet nozzles were tested on a comparative basis. In accordance with [2], the radius of curvature of these inlet nozzles was selected such that its ratio to the impeller inlet diameter (r_D/D_S) was equal to about 0.14. Wheel nozzles employed were of a conventional type fabricated according to current engineering literature. These nozzles were then modified to match the requirements of the specific inlet configuration. In this context, special importance was attached to the influence of the gap width s and the gap overlap x on the fan's characteristic curves.

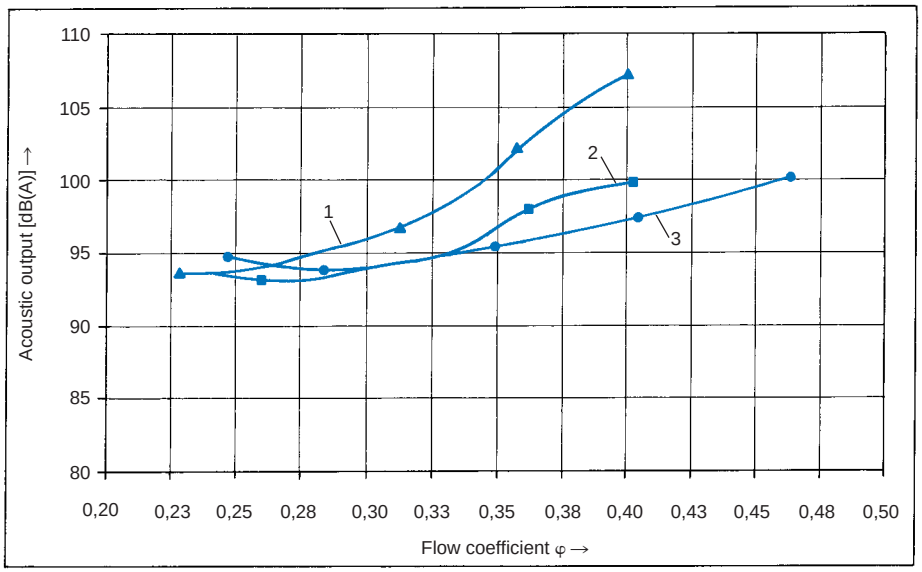

Fig. 13: Comparison of ER 30/3.5 acoustic emissions with impellers from diverse manufacturers (rpm adjusted to the same operating point)
1) Reference impeller 1
2) Reference impeller 2
3) ER 30/3.5

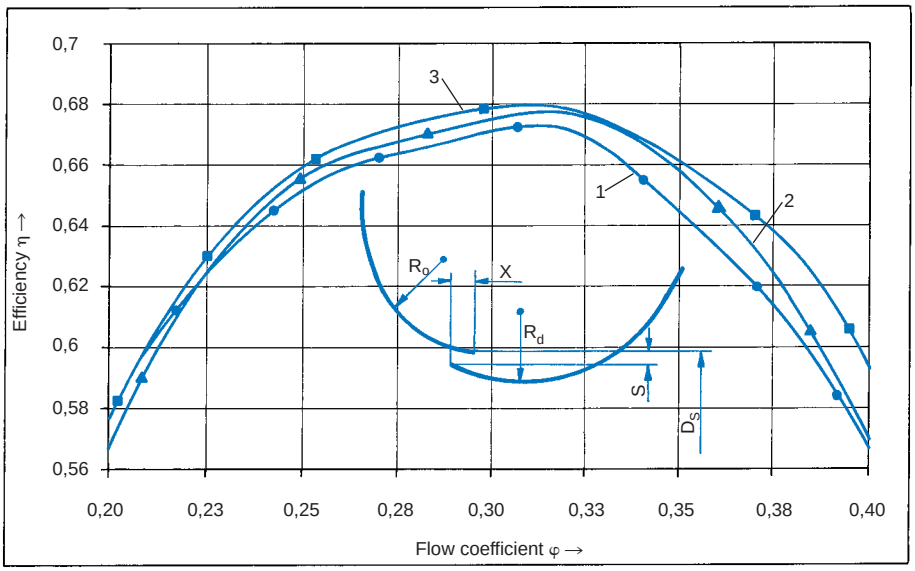

Fig. 14: Efficiency characteristic versus flow coefficient
1) Conventional impeller inlet with r_D/D_S = 0.14, s/D_S = 0.014, x/D_S = 0.014
2) Expanded impeller inlet with r_D/D_S = 0.14, s/D_S = 0.007, x/D_S = 0.014
3) Expanded impeller inlet with r_D/D_S = 0.14, s/D_S = 0.007, x/D_S = 0.04

Result

Fig. 14 shows the plots for three different impeller inlet nozzles. They all share the same r_D/D_S (impeller radius of curvature to inlet diameter) ratio of 0.14. The first nozzle is a conventional, commercially available inlet unit fabricated as prescribed in the specialized literature. The characteristic curve shows the least favourable pattern in this case.

In a second trial, an inlet nozzle of the same design was used but optimized by expansion to increase the gap impulse and hence, the gap velocity. As can be seen from the diagram, this approach gave a slightly increased efficiency and flow coefficient. An even greater increase in these parameters was obtained in the third trial, where the gap overlap (Fig. 7) was adapted in addition to the gap width.

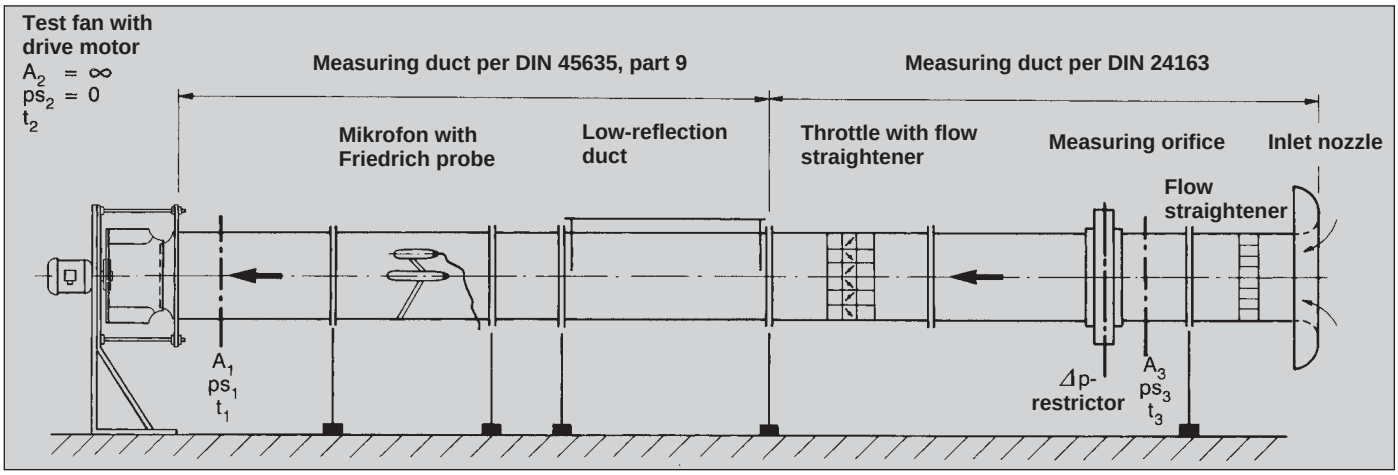

Bild 15: TLT test rig according to DIN 45635, Part 9, and DIN 24163

TLT test-rig measurements

The test rig employed at TLT meets DIN 24 163, Part 2, standard specifications for volume flow and pressure measurements, and DIN 45 635, Part 9, for sound measurements.

Pressure-versus-volume-flow characteristics of the plug-in fan centrifugal fan were determined on our standard-compliant test rig by intake-side throttling.

The test-rig configuration was of the intake-side airway type depicted in Fig. 15. It ensures a swirl-free, uniform incoming airflow at each operating point of the fan's characteristic curve and hence, repeatable readings.

The sound output emitted into the ducting by the fan is recorded by the in-duct measuring method using a microphone mounted on a so-called Friedrich probe [4, 5].

Literature

[1] Kaup C.: Einsatz von freilaufenden Rädern als Ventilatorsystem in RLT-Geräten [Use of plug-in fan impellers as a fan system in AHU equipment], HLH 47 (1996), No. 8, p. 34-38

[2] Bommes L.: Problemlösungen bei der Gestaltung von Radialventilatoren [Solutions to problems encountered in centrifugal fan design), HLH 25 (1974), No. 12, p. 420-425

[3] Leist H., Roth H.W., Schilling R., Zierep J: Neuere Entwicklungen auf dem Gebiet der Radialventilatoren hoher Leistungsdichte [Recent developments in centrifugal fans of high power density], HLH 30 (1979), No. 11, p. 443-447

[4]DIN 45635, Measurement of noise emitted by machines, Part 9.

[5] DIN 24163, Fans; performance testing, standardized test airways, Part 2.

11